Fairness Analysis of Physical Layer Capture Effects in IEEE 802.11 Networks

Yigal Bejerano
Bell Labs, Alcatel-Lucent
Murray Hill, NJ, USA
bej@research.bell-labs.com

Hyoung-Gyu Choi
Department of Computer Science
Yonsei University, Seoul, Korea
hgchoi@cs.yonsei.ac.kr

Seung-Jae Han
Department of Computer Science
Yonsei University, Seoul, Korea
sjhan@cs.yonsei.ac.kr

***Abstract*—Physical layer capture is one of the main causes of unfairness in IEEE 802.11 Wireless LANs. While existing work have analyzed the impact of physical layer capture on the total system throughput of a cell, we analyze the unfairness among users as result of capture. Since this unfairness is related to the relative location of users, we call it as *spatial unfairness*. Our analysis characterizes the relative throughput share of a user as a function of the users' distance from the Access Point (i.e., as a function of received signal strength). We validate the accuracy of our analysis via extensive simulations and experimental measurements.**

I. Introduction

The MAC (Medium Access Control) protocol of IEEE 802.11 Wireless LAN is designed to provide long-term fairness even when stations use different transmission bit-rates. Such long-term fairness is experimentally demonstrated in [1]. In this experiment, however, all users have about the same signal strength while they use different transmission bit-rates. In reality, the long-term fairness of IEEE 802.11 WLAN is not guaranteed when stations have different signal strengths, even if they use the same transmission bit-rate. Depending on the signal strength (i.e., user distance from the AP), severe long-term unfairness can occur because of the *physical layer capture* (or *capture effect*).

The capture effect causes unfairness as some packets are correctly decoded while other packets cannot be decoded upon the collision between simultaneously transmitted packets. In general, if the signal strength of a packet is substantially higher than that of another packet, the stronger packet can be correctly received despite the collision. Thus, the stronger signal user will get higher throughput than the weaker signal user. After a packet loss, IEEE 802.11 MAC slows down the channel access attempts by increasing the size of the contention window, which further aggravates the unfairness. Unfairness due to the capture effect occurs when several stations simultaneously attempt to send packets to a common *access point* (AP). On the other hand, the capture effect has a positive side from the viewpoint of total system throughput. It is because some transmissions become successful even if collisions do occur, reducing the waste of link resources upon collisions thanks to the capture effect. Some studies [2], [3] leverage this phenomena to enhance the system throughput.

The impact of capture effect on the total system throughput is mathematically analyzed in many papers. In [5], Chang et al. present an analytic model that computes the system throughput by treating the capture effect as a consequence of interferences. They model the packet error probability by using interference relations among neighbor nodes. In [6], the capture probability is computed by comparing the power of a received frame with the joint power of interfering contenders. In [7], [8], [9], [10], the packet loss probability is modeled in a similar manner to [6]. Commonly in these papers, the packet loss probability is estimated by extending the model proposed in [4] to reflect the probability of capture effect.

The fairness issue of physical layer capture has received relatively little attention, despite early recognition of this issue in [11]. This aspect has been mostly studied experimentally [12], [13], [14], [15], [16]. A particularly useful result is reported in [14], which demonstrates that the frame with the stronger signal is captured regardless of its timing with respect to the preamble of the weaker signal frame. Unlike the existing studies, we focus on *rigorous analysis for explicitly characterizing the unfairness caused by physical layer capture*. To the best of our knowledge, only [17] attempts to tackle this problem, which first used the term *spatial unfairness* to denote the throughput unfairness caused by the relative location of the users that are connected to the same AP. The study, however, makes several simplifying assumptions that hinder the accurate analysis. For instance, it consider a simple wireless channel model, which ignores fast-fading effects, and it assumes unbounded interference range.

To analyze spatial unfairness we model the interaction between the physical capture effects and IEEE 802.11 MAC. Our mathematical model characterizes the spatial unfairness when the network is operating in the saturated mode. The spatial unfairness may be affected by other factors such as the used higher layer protocols and hidden nodes. The impact of these factors is beyond the scope of this paper. For instance, while different higher layer protocols might affect the spatial unfairness in a different manner, we consider only UDP traffic.

Our contributions are as follows.

1. In Section III, we investigate the characteristics of spatial unfairness experimentally. Since several studies have already experimentally demonstrated the impacts of capture effect, we demonstrate that spatial unfairness may occur even when only two users are associated with an AP.

2. In Section IV we present an analytical model to estimate the spatial unfairness as a function of the received signal strength indicator (RSSI). More specifically, we estimate the normalized bandwidth of each station relative to the average bandwidth, for any arbitrary distribution of user locations. In

978-3-9018-8273-9/15/ ©2015 IFIP

Section V we validate our theoretical model by using the results of our two user experiments.

3. Section VI describes our simulation results under various settings, including different number of users and various capture thresholds. We show that user throughput can change widely even if all users use the same transmission bit-rate. Due to space limit, only selected simulation results are presented.

II. Network Model

No Inter-cell Interference - We assume a WLAN with proper frequency planning such that adjacent APs do not interfere to each other. This allows us to consider each AP as an individual WLAN that serves N static users. The AP has a transmission range (or cell radius) R and we denote by d_i the distance between the AP and any user $i \in \{1, \cdots, N\}$ $d_i < R$. The vector $\vec{d} = \{d_1, \cdots, d_N\}$ represents the distance of each user from the AP. We assume that all the users can hear each others' transmissions, i.e., no hidden terminals.

IEEE 802.11 MAC - We consider WLAN operates in infrastructure mode. All stations (both AP and users) use the standard IEEE 802.11 MAC protocol [18]. Each station senses the channel before transmission. It starts transmission only if the channel is idle for a backoff duration, measured in time *slots*, which is randomly chosen according to the user's *contention window (CW)* variable. If it senses a busy channel during its backoff duration, it freezes its backoff timer and resumes the timer again at the end of the sensed transmission. A user transmits its packet only when its backoff timer expires. At the end of each successful transmission, the receiving station acknowledges the reception by sending an ACK message. Collisions occur as a result of several users transmitting simultaneously. If a station does not receive an ACK, it doubles its contention window size up to a maximal CW value denoted by $CW_{max} = 2^K \cdot W$, where W (also denoted as CW_{min}) is the minimum contention window size and K is a constant integer. The user resets its contention window size to its initial value, W, after every successful transmission.

Wireless Channel Model - We adopt a *conventional wireless channel model*, as described in [19], [20], [21]. We assume that all the users transmit with the same transmission bit-rate, b, and power, P_0. The received signal strength depends on channel attenuation and shadowing affects. More specifically, for a receiver at distance d from a sender, the received power is calculated as follows;

$$Pr(d) = \frac{P_0 \cdot G}{d^\alpha} \cdot \mathcal{Y}_\sigma \quad (1)$$

where the *attenuation exponent*, α, (typically in the range $[2, 4]$) is a constant that depends on the characteristics of the transmission environment. G is the processing gain, and $\mathcal{Y}_\sigma$ is a log-normal random variable (r.v.) with location parameter $\mu = 0$ and scale parameter σ. Recall that the received power can be represented in dB as follows:

$$Pr(d)[dB] = 10 \cdot [\log P_0 + \log G - \alpha \cdot \log d + \log e \cdot \mathcal{X}_\sigma] \quad (2)$$

where $\log$ is the logarithm with base 10 and $\mathcal{X}_\sigma = \ln \mathcal{Y}_\sigma \sim \mathcal{N}(0, \sigma^2)$ is normal r.v. with mean $\mu = 0$ and standard deviation σ. For successful decoding at transmission bit rate b, the *signal to noise ratio (SNR)* at the receiver side should be above a certain *SINR threshold*, denoted by H_b.

$$SINR = \frac{Pr(d_s)}{BN_0 + \sum_{i \in IS} Pr(d_i)} \geq H_b \quad (3)$$

BN_0 indicates the background noise like thermal noise. d_s is the distance between the receiver and the transmitter. d_i is the distance between the receiver and an interfering node i at the interference set IS. Since the probability of three or more simultaneous transmissions is typically low, we consider the case of at most two simultaneous transmissions. We also ignore the background noise which is very low. In such case, SINR is given by the following equation;

$$SINR(d_s, d_i) = \frac{Pr(d_s)}{Pr(d_i)} \geq H_b \quad (4)$$

Table I summarizes the key notations. Note that in general the parameters π, p_{tx} and q depend on the vector $\vec{d}$.

Symbol	Semantics
N	The number of users associated with the AP.
d_i	The distance (meters) between user i and the AP.
$\vec{d}$	A vector of distances between the users and the AP.
$Pr(d)$	The received signal strength at distance d.
P_0	The transmission power of all the stations.
α	The *attenuation exponent*.
H_b	Minimal SINR for communicating at bit-rate b.
W	The minimal contention window size, i.e., CW_{min}.
K	Num. of CW duplications, *i.e.*, $CW_{max} = CW_{min} \cdot 2^K$.
$\pi(d_i)$	The probability of successful transmission of user i with distance d_i from the AP at any slot.
$p_{tx}(d_i)$	The probability of a transmission of user i at any slot.
$q(d_i)$	The failure probability (collision) for user i.

TABLE I: Notations.

III. Experimental Evaluation of Spatial Unfairness

A. Two Types of Collision

We start with a brief explanation of spatial unfairness due to capture, similar to the one given in [17]. Consider a collision between two simultaneously transmitted packets to the AP. There are two possible outcomes of the collision, depending on the Received Signal Strength Indication (RSSI) of the two packet transmissions at the AP.

Case I: Comparable RSSI – Eq. (4) suggests that the AP can decode a packet only if its SINR is above a certain threshold H_b. If the RSSI at the AP of the two packets that collide are comparable, the AP cannot decode either of the packets. Since no acknowledgement is received, both users infer a collision and increase their contention windows before the retransmission. In this scenario, the two users get roughly the same throughput.

Case II: Disparate RSSI – Consider a scenario in which the RSSI at the AP of one user is significantly higher than the RSSI of the other user. Despite the collision, the SINR of the near user's packet at the AP could be above H_b, which allows the

AP to decode its packet. We refer to such situation as *capture*. Capture leads to throughput unfairness between the near user and the far user. This unfairness is aggravated by the backoff mechanism of DCF MAC. The user with stronger RSSI does not identify the collision and it keeps its contention window at default value, i.e., CW_{min}. However, the user with weaker RSSI does not receive ACK and assumes collision which doubles the size of its contention window. Since the contention window of a node is used to determine its backoff time, the result is that the stronger user will get more transmission attempts than the weaker user.

B. Experiment Setting

We validate the presence of spatial unfairness via experiments.The experiments are carried out in an indoor testbed with a single 802.11a WLAN cell containing two user terminals. The AP and the terminals are notebook computers running Redhat Linux 4.1.0 (2.6.15 kernel) with Cisco Aironet 802.11 a/b/g adapter [22]. Madwifi version 0.9.4 driver is used. The main parameters for our experiments are as follows;

- Minimal contention window, $CW_{min} = 4$.
- Maximal contention window, $CW_{max} = 256$.
- Transmission power of all stations, $P_0 = 10dBm$,
- Fixed transmission bit-rate of 24 $Mbps$.
- Fixed packet size of 1375 bytes.

Users were positioned at five carefully-selected locations (referred to as 'Loc 1', 'Loc 2', ..., 'Loc 5'), so that they experience sufficiently different channel quality (i.e., different RSSI measured at the AP). The RSSIs at two adjacent locations are about 6 dB apart from each other. Since the cell contains two users, we deliberately select a very small $CW_{min} = 4$. As a result, the chance of collision is approximately 25%. In the real world environments, CW_{min} may be set to a larger value, but in such cases the number of contending users may also be larger. We used fixed transmission bit-rate of 24 $Mbps$ regardless of the location of users for eliminating uncontrolled effects of bit-rate adaptation. To avoid the influence of high layer protocols, which is not considered in this paper, only UDP traffic is generated by using *iperf 2.0.4*. All the UDP packets have the same size of 1375 bytes. For creating collisions, uplink traffic is sent by user terminals to the AP at a rate high enough to saturate the MAC sender queue (i.e., queue never becomes empty). The RTS/CTS feature is disabled. We conducted the experiment during late night when interference from other sources are negligible.

To obtain the base line performance, we first conduct measurement with a single user. Note that no collision occurs in this setting. The measurement results are summarized at Table II. Each value is obtained by averaging the results of 10 experiments. At all the locations, except 'Loc 5', the retry rate was negligible and the same throughput was measured, which implies that *the AP can decode almost all packets sent from these locations, if there are no collisions.* The high retransmission rate at Loc 5 suggests that SINR at Loc 5 is marginal to support the 24 Mbps transmission mode. Therefore, for our unfairness analysis, we consider only Loc 1-4, where all packet retransmissions are caused by collisions.

TABLE II: Baseline measurement (one user experiment)

	Throughput (Mbps)	SINR (dB)	Transmission mode (Mbps)	Retransmission ratio (%)
Loc 1	18.0	52	24	0
Loc 2	18.0	44	24	0
Loc 3	18.0	40	24	0
Loc 4	18.0	34	24	0
Loc 5	15.3	27	24	13

C. Experiment Results

Now, we conduct two user experiments. The user nearer to the AP is called the *Near user* (denoted as *NU*) and the user farther from the AP is called the *Far User* (denoted as *FU*). We test all possible location combinations. The observed throughput and the corresponding retransmission ratio of the users at seven different NU-FU locations are presented in Figure 1 and Figure 2, respectively.

The main observations are as follows. When both user were placed at the same location (e.g., Loc $1-1$), they experience similar retransmission ratio and consequently similar throughput of about 8 $Mbps$. As FU moves away from the AP while NU stays at Loc 1 (i.e, the first four cases in the graphs), NU's throughput increases while FU's throughput stays roughly the same. It is mainly because NU's retransmission rate decreases thanks to the capture effect, while the retransmission rate of the FU does not change. When FU locates at Loc 4, NU's retransmission ratio is near zero and FU's retransmission ratio is about 25%. In this case (i.e., Loc $1-4$), the NU's throughput is 10.2 $Mbps$ and the FU's throughput is 8.2 $Mbps$, which clearly indicates the presence of spatial unfairness. Since the retransmission ratio is near zero, NU's CW size will stay at the minimal value unlike the other cases where NU's average CW size will be higher than the minimal value.

Next, we place NU at Loc 2. If FU is at Loc 2, a very similar result as the case of Loc $1-1$ is observed. The results for the same location case except Loc $1-1$ are omitted in Figure 1 and Figure 2. While FU is at Loc 3 (i.e., Loc $2-3$, a similar results as Loc $1-2$ is observed (i.e., slight spatial unfairness). This is because the SINR gap between Loc 2 and 3 is $46-40 = 6$ dB (see Table II), while the SINR gap between Loc 1 and 2 is also 6 dB. The degree of spatial unfairness increases as FU moves to Loc 4 (i.e., Loc $2-4$). Finally, we can observe slight spatial unfairness in case of Loc $3-4$, as expected. This is because some of retransmissions of FU result from the poor channel condition of the FU (as shown in the last row of Table II).

The experimental results provide a strong indication of spatial unfairness, which depends on the SINR difference as well as the minimal contention window, CW_{min}.

IV. Fairness Analysis

In this section we mathematically analyze the impact of physical layer capture on the fairness of the services that an AP provides to its associated users. Note that the capture effect impacts only upstream traffic (i.e., traffic from the users to the AP), so our analysis considers only upstream traffic.

The impact of physical layer capture depends on many factors such as channel condition, traffic load, and modulation

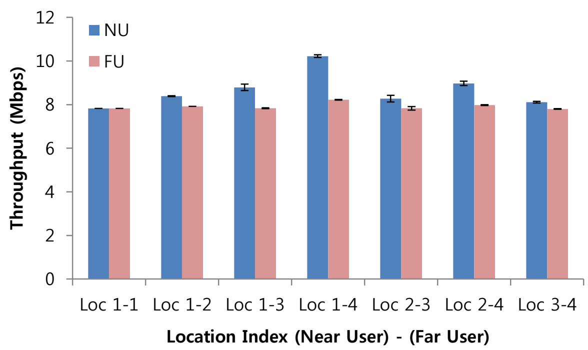

Fig. 1: Throughput comparison (two user experiments).

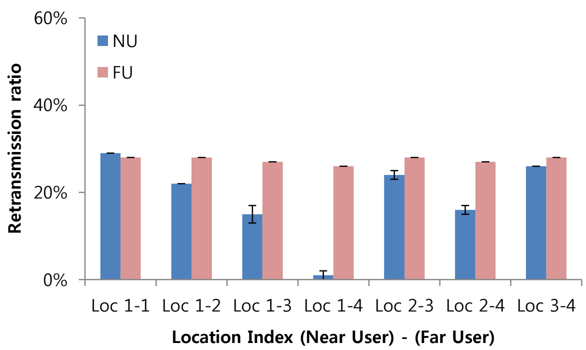

Fig. 2: Retransmission rate comparison (two user experiments).

scheme. To make the analysis mathematically feasible, we conduct a *saturation mode* analysis, in which all the users always have data to transmit to the AP, therefore contend for the channel at all times, while the AP does not send any downlink traffic. We assume that all the users use the same transmission bit-rate[1], denoted by b, and the packet sizes are *constant* and *equal* for all users. In our analysis packets are lost only due to collisions and we ignore channel errors[2].

A. Objective and Methodology

Our objective is to analyze the spatial unfairness. As Eq. (1) indicates, the channel quality of a user decreases with its distance from the AP. Our analysis estimates the *normalized bandwidth* (NBW) that a user s with distance d_s from the AP experiences relative to the average bandwidth (i.e., throughput) of all the users. Let $BW(d_s, \vec{d})$ represent the bandwidth received by user s, while $\vec{d} = \{d_1, \cdots, d_N\}$ denotes the distance vector of all the users. The normalized bandwidth, $NBW(d_s, \vec{d})$, of user s is defined as follows;

$$NBW(d_s, \vec{d}) = \frac{BW(d_s, \vec{d})}{E\{BW(d_j, \vec{d})\}} = \frac{\pi(d_s, \vec{d})}{E\{\pi(d_j, \vec{d})\}} \quad (5)$$

We calculate $NBW(d_s, \vec{d})$ indirectly by evaluating the *probability of successful transmission of user s at any slot*, termed the *successful transmission probability* of user s and denoted by $\pi(d_s, \vec{d})$. Obviously, $BW(d, \vec{d}) \propto \pi(d, \vec{d})$ and therefore $NBW(d_s, \vec{d})$ can be calculated by using Eq. (5).

[1]Our analysis can be easily extended to the case where users have varying packet sizes and transmission rates.

[2]While we do not include channel error in this study, our analysis can accommodate channel error in the same way as in [7].

The physical meaning of Eq. (5) is as follows, which is the central formula for our analysis. Since we assume that all data packets have the same length, the experienced bandwidth of a user is proportional to the number of its successful transmission. So, our analysis boils down to estimating the fraction of slots in which a user has successful transmissions and comparing this fraction against the average successful transmission probability. For example, consider a WLAN with two users 1 and 2 (with distance d_1 and d_2 from the AP, respectively) and let assume that $\pi(d_1) = 15\%$ while $\pi(d_2) = 5\%$. Thus, $E\{BW(d_j, \vec{d})\} = (15\% + 5\%)/2 = 10\%$. By using Eq. (5), we see the $NBW(d_1, \vec{d}) = 15\%/10\% = 1.5$ while $NBW(d_2, \vec{d}) = 5\%/10\% = 0.5$. This means that user 1 has 50% higher throughput than the average, while the bandwidth of user 2 is only half of the average.

B. Calculating the Successful Transmission Probability

We now provide a general framework for calculating the successful transmission probability at any slot, $\pi(d_s, \vec{d})$, of any sender s, among the N users associated with the AP. $\pi(d_s, \vec{d})$ depends on the probability that user s makes a transmission attempt at any slot, denoted by $p_{tx}(d_s, \vec{d})$ and the probability that an individual transmission is successful. We denote the failure probability by $q(d_s, \vec{d})$.

$$\pi(d_s, \vec{d}) = p_{tx}(d_s, \vec{d}) \cdot [1 - q(d_s, \vec{d})] \quad (6)$$

Since we consider static users operating in the saturation mode, the transmission rate and the failure probability of a user are time-invariant and are proportional to the level of contention experienced by the user. This is a common assumption made by the most relevant studies, e.g., [4]. Consequently, p_{tx} and q parameters of a user depend only on its distance from the AP and the other users' distribution. For our analysis we leverage the prominent result of Bianchi in [4] that provides a simple and accurate relationships between p_{tx} and q.

$$p_{tx}(q) = \frac{2}{1 + W + q \cdot W \cdot \sum_{j=0}^{K-1} (2 \cdot q)^j} \quad (7)$$

Although in [4], it is assumed that all the users have the same transmission prob. and experience the same failure prob., unlike our study, Eq. (7) is valid also in our case. Observe that Eq. (7) considers a single user and provides the relation between the prob. of user transmission attempt at any slot for any given failure prob., q. Thus, even when the users experience different failure prob., $q(d_i, \vec{d})$, as in our analysis, the relationship between the q and p_{tx} parameters of the different users, as represented by Eq. (7), is still valid.

The received signal strength at the AP is different for different users. From Eq. (4), it follows that a transmission of a sender s collides with a packet of an interfering node i w, only if $SINR(d_s, d_i) = \frac{Pr(d_s)}{Pr(d_i)} < H_b$, where d_s and d_i are the distance from the AP to s and i, respectively. Hence the failure probability of a sender s can be formulated as follows:

$$q(d_s, \vec{d}) = 1 - \prod_{i=1, i\neq s}^{N} [1 - p_{interfr}(d_s, d_i)] \tag{8}$$

In Eq. 8, $p_{interfr}(d_s, d_i)$ is the *interference probability* that the transmission of user i interferes with the transmission of sender s. For any $i \neq s$, $p_{interfr}(d_s, d_i)$ can be calculated from Eq. (9), in which $Prob\{SINR(d_s, d_i) < H_b\}$ is that the SINR of the transmission of user s is below the SINR threshold H_b due to simultaneous transmission of node i. $Prob\{SINR(d_s, d_i) < H_b\}$ is essentially the *collision failure probability*, which is calculated in Section IV-C.

$$p_{interfr}(d_s, d_i) = p_{tx}(d_i, \vec{d}) \cdot Prob\{SINR(d_s, d_i) < H_b\} \tag{9}$$

Since we assume any arbitrarily vector $\vec{d}$, there is no close form solution to Eq. (8) and (9). q and p_{tx} parameters of all the users need to be solved numerically in a iterative manner, as described later.

C. Estimating the Collision Failure Probability

Consider a sender s and an interfering node i with distances d_s and d_i from the AP, accordingly. We use Eq. (2) for calculating the collision failure probability.

$$\begin{aligned} SINR(d_s, d_i)[dB] &= Pr(d_s)[dB] - Pr(d_i)[dB] = \\ &= 10 \cdot [\log P_0 + \log G - \alpha \cdot \log d_s + \log e \cdot \mathcal{X}_{s,\sigma}] \\ &\quad - 10 \cdot [\log P_0 + \log G - \alpha \cdot \log d_i + \log e \cdot \mathcal{X}_{i,\sigma}] \quad (10) \\ &= 10 \cdot [\alpha \cdot (\log d_i - \log d_s) + \log e \cdot (\mathcal{X}_{i,\sigma} - \mathcal{X}_{s,\sigma})] \end{aligned}$$

This means that

$$Prob\{SINR(d_s, d_i)[dB] < H_b[dB]\} = \tag{11}$$

$$Prob \left\{ \mathcal{X}_{i,\sigma} - \mathcal{X}_{s,\sigma} < \frac{H_b[dB]/10 + \alpha \cdot (\log d_s - \log d_i)}{\log e} \right\}$$

For simplifying the notations, we define,

$$g_b(r_s, r_i) = \frac{H_b[dB]/10 + \alpha \cdot (\log d_s - \log d_i)}{\log e} \tag{12}$$

Let $\mathcal{Z} = \mathcal{X}_{i,\sigma} - \mathcal{X}_{s,\sigma}$. R.v. $\mathcal{Z}$ is the summation of two normal r.v. with mean $\mu = 0$ and standard deviation σ. $\mathcal{Z}$ has a normal distribution with mean 0 and standard deviation $\sigma_{\mathcal{Z}} = \sqrt{2} \cdot \sigma$, i.e., $\mathcal{Z} \sim \mathcal{N}(0, 2 \cdot \sigma^2)$. Let $\phi(x) = \int_{-\infty}^{x} \frac{1}{\sqrt{2\Pi}} \cdot e^{-\frac{x^2}{2}} dx$ denotes the CDF of the standard normal distribution. From the above discussion, it results that,

$$Prob\{SINR(d_s, d_i) < H_b\} = \tag{13}$$

$$Prob\{Z < g_b(r_s, r_i)\} = \phi\left(\frac{g_b(r_s, r_i)}{\sqrt{2} \cdot \sigma}\right)$$

D. The Iterative Process

We now present a simple iterative process for calculating the transmission probability, $p_{tx}(d_i, \vec{d})$ and failure probability $q(d_i, \vec{d})$ of each user s.

Initialization: We initialize the $p_{tx}^0(d_s, \vec{d})$ and $q^0(d_s, \vec{d})$ parameters of each user s by using Bianchi scheme [4], assuming that all users experience the same failure probability. The initial values are calculated iteratively by using the relation,

$$q = 1 - [1 - p_{tx}(q)]^{N-1}$$

This equation is a direct result from Eq. (8) and Eq. (9) when assuming that any two simultaneous transmissions collide.

Iterative Step: At each iteration t, we use the transmission probabilities $p_{tx}^{t-1}(d_s, \vec{d})$ from the previous iteration, $t-1$, as input for Eq. (8) and Eq. (9) for calculating temporary failure probabilities $q^{tmp}(d_s, \vec{d})$ for each user s. Then, the failure probability of each user is calculated by taking the average of q^{t-1} and q^{tmp};

$$q^t(d_s, \vec{d}) = (q^{t-1}(d_s, \vec{d}) + q^{tmp}(d_s, \vec{d}))/2 \tag{14}$$

Since p_{tx} is inversely proportional to q (as shown in Eq. (7)), oscillations due to over or under estimation of these two parameters may be avoided by taking the average between q^{t-1} and q^{tmp}. Then, the transmission probability, $p_{tx}^t(d_s, \vec{d})$ is calculated for each user by using Eq. (7).

Termination: The iterative process terminates when the maximal change of the failure probability, q, is below a given threshold, e.g., $\Delta = 10^{-6}$. Then, we use Eq. (6) to calculate the successful transmission probability, $\pi(d_s, \vec{d})$, of each user s and its normalized bandwidth $NBW(d_i, \vec{d})$.

E. The Case of Uniform User Distribution

We now consider the case of uniform user distribution and calculate the successful transmission probability $\pi(d)$ for any distance d from the AP, when the number of users N and the minimal SINR threshold H_b are given. Since the users locations are unknown, we cannot use Eq. (8) and Eq. (9). We can only approximate the probabilities $q(d)$, $p_{tx}(d)$ and $\pi(d)$ for any distance d from the AP.

To this end, we assume a transmission of user s with distance d_s from the AP and consider the probability, $\hat{p}_{interfr}(d_s)$, that any other user interferes this transmission. The probability $\hat{p}_{interfr}(d_s)$ of Eq. (15) is calculated similarly to Eq. (9).

$$\hat{p}_{interfr}(d_s) = \int_0^R \frac{2 \cdot r}{R^2} p_{tx}(r) \cdot Prob\{SINR(d_s, r) < H_b\} dr \tag{15}$$

The main difference between the two equations is that $\hat{p}_{interfr}(d_s)$ assumes an arbitrate user at any location. Since we assume uniform user distribution, the probability that a user is located with distance r from the AP is given by $\frac{2\Pi r dr}{\Pi R^2} = \frac{2rdr}{R^2}$. Consequently, Eq. (8) can be simplified and the failure probability $q(d_s)$ of user s is computed by using Eq. (16).

$$q(d_s) = 1 - [1 - \hat{p}_{interfr}(d_s)]^{N-1} \tag{16}$$

In our iterative process, the integral of Eq. (15) is approximate with a summation.

V. Validation of the Analytical Model

This section validates the correlation between our analytical model presented in Section IV and the experiment results presented in Section III. To this end we compare the *collision-failure-ratio* (CFR) obtained from the experiments with that calculated by our model. CFR is the ratio of collision failures of the Near User (NU) relative to the Far User (FU). CFR is a proper metric for evaluating the unfairness between users since it compares the packet loss ratio of the users. For instance, a CFR of 0.5 implies that FU suffers twice as many losses than NU. We assume all losses are caused only by collisions.

We first calculate the *collision failure probability* of a user u_s due to the collision with a user u_i as follows

$$P_{failure}(u_s, u_i) = Prob\{SINR(u_s, u_i) < H_b\}.$$

$P_{failure}(u_s, u_i)$ is expressed as a function of the users' received signal strength indicator (RSSI) at the AP. By using similar relation to Eq. (2), the RSSI of user u can be expressed as follows

$$Pr(u)[dB] = \hat{Pr}(u)[dB] + 10 \cdot \log e \cdot \mathcal{X}_\sigma,$$

$\hat{Pr}(u)[dB]$ is the average RSSI of user u at the AP in the unit of dB. Using this formula, Eq. (10) can be written as

$$SINR(u_s, u_i)[dB] = \Delta Pr[dB] + 10 \cdot \log e \cdot (\mathcal{X}_{s,\sigma} - \mathcal{X}_{i,\sigma})$$

given that $\Delta Pr = \hat{Pr}(u_s)[dB] - \hat{Pr}(u_i)[dB]$ is the average RSSI discrepancy between the users. By using this relation, Eq. (11) can be written as

$$P_{failure}(u_s, u_i) = Prob\{SINR(u_s, u_i)[dB] < H_b[dB]\} = Prob\left\{\mathcal{X}_{s,\sigma} - \mathcal{X}_{i,\sigma} < \frac{H_b[dB] - \Delta Pr[dB]}{10 \cdot \log e}\right\}. \quad (17)$$

Finally, the CFR of a given NU-FU pair is formally defined as follows

$$CFR(NU, FU) = \frac{P_{failure}(NU, FU)}{P_{failure}(FU, NU)}. \quad (18)$$

CFR depends on ΔPr, a scale parameter σ for the log-normal r.v. and SINR threshold H_b.

Now, by using Eq. (17) and Eq. (18), we calculate the CFR with the ΔPr values used in the experiments. Table III show the $CFR(NU, FU)$ computed by our analytical model for $\Delta Pr = \{0\ dB, 6\ dB, 12\ dB, 18\ dB\}$, which are the RSSI gaps between the user locations in the experiment. We use the transmission bit-rate of 24 $Mbps$ in the experiments. From [22] we found that the receive sensitivity of 802.11a Aironet adaptor is typical $-82dBm$ for bit-rate of 24 $Mbps$. Given floor noise around $-95dBm$, the SINR threshold for bit-rate of 24 $Mbps$ becomes $H_b = 13\ dB$. We have tried various $\sigma = \{0.6, 0.8, 1.0, 1.2\}$.

We then derive the CFR from our experiment results. Recall that all retransmissions are caused by collision with the user locations (except 'Loc 5') in our experiments. We calculate the total number of failed transmissions of a user u as follows[3],

$$Failures(u) = \frac{Successful\_trans(u)}{1 - retry(u)} \cdot retry(u) \quad (19)$$

[3]Note that the ratio of the retry rates of the users cannot be used as CFR, since the users may have different number of successful transmissions.

TABLE III: CFR computed by using our analytical model

ΔPr	$\sigma = 0.6$	$\sigma = 0.8$	$\sigma = 1.0$	$\sigma = 1.2$
0	1.00	1.00	1.00	1.00
6 dB	0.97	0.92	0.86	0.83
12 dB	0.61	0.58	0.56	0.55
18 dB	0.08	0.15	0.20	0.25

TABLE IV: CFR measured in our experiments

↓ NU, FU →	Loc-1	Loc-2	Loc-3	Loc-4
Loc-1	1.05	0.77	0.53	0.04
Loc-2	-	-	0.86	0.58
Loc-3	-	-	-	0.94

$Successful\_trans(u)$ is derived from the throughput of user u and $retry(u)$ is the retransmission rate of user u which can be directly measured. Since all the packet losses are resulted from collisions, it implies that the ratio $\frac{Failures(NU)}{Failures(FU)}$ is indeed the $CFR(NU, FU)$. Table IV show the $CFR(NU, FU)$ obtained from our experiments. Recall that the RSSI gap between adjacent locations is about 6 dB.

Several observations are possible from the two tables. First, when both users are at Loc-1, the CFR measured in experiments is 1.05. This corresponds to the case of $\Delta Pr = 0$ in Table III. As two users experience the same RSSI, their collision failure probabilities should be very similar.

Second, consider the RSSI gap between the two users is about 12 dB: (i) the case of NU at Loc-1 and FU at Loc-3, (ii) the case of NU at Loc-2 and FU at Loc-4. In these cases, $CFR \approx 0.55$, which agrees well with the row of $\Delta Pr = 12\ dB$ in Table III. This also strongly supports that the estimation of SINR threshold $H_b = 13\ dB$ by our analytical modeling is correct.

Third, for a given ΔPr, CFR tends to increase with the distance (i.e. with the reduction of RSSI). Compare the case of Loc 1-2, Loc 2-3 and Loc 3-4 in Table IV. Though $\Delta Pr = 6\ dB$ in all three cases, the CFR of Loc 2-3 is bigger than that of Loc 1-2, and the CFR of Loc 3-4 is bigger than that of Loc 2-3. To explain this phenomenon, we need to revisit Eq. (3), which shows that the SINR depends not only on ΔPr but also on other aspects such as the background noise BN_0. The impact of these extra components on the SINR increases as the RSSI of the NU and FU decrease together (e.g., in case of Loc 3-4). In Table II, it is shown that at Loc-5 (with SINR of 27 dB above the background noise) the user suffers from retransmission rate 13% due to the background interference. This implies that *we cannot find a single scale parameter σ that fits all the experiment results.*

Fourth, although there is no single σ that can be used for all cases, we observe that $\sigma = 0.8 \pm 0.2$ provides a good agreement between the experiment results and the modeling results. Tables IV and III show strong correlation, which validate our mathematical model presented in Section IV. We use this information to infer the wireless channel characteristics for our simulations, presented in Section VI.

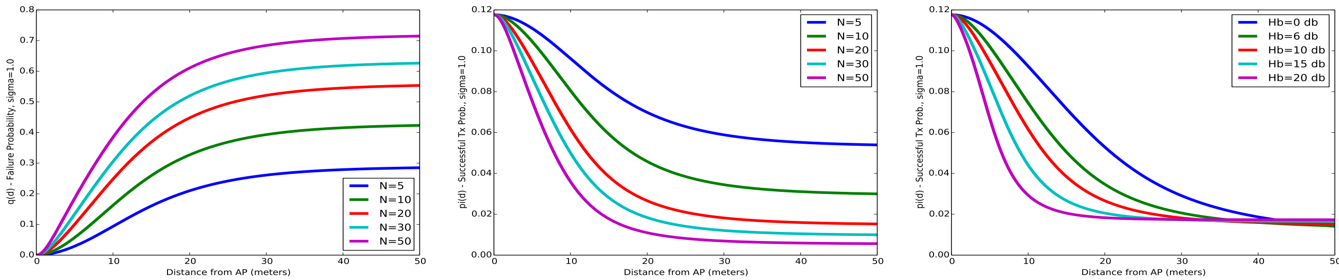

(a) Failure prob. for different number of users, $H_b = 10\ dB$ and $\sigma = 1.0$.

(b) Successful trans. prob. for different number of users, $H_b = 10\ dB$ and $\sigma = 1.0$.

(c) Successful trans. prob. for different H_b thresholds, $N = 20$ and $\sigma = 1.0$.

Fig. 5: Failure probability, $q(d)$, and Successful transmission probability, $\pi(d)$, for different settings.

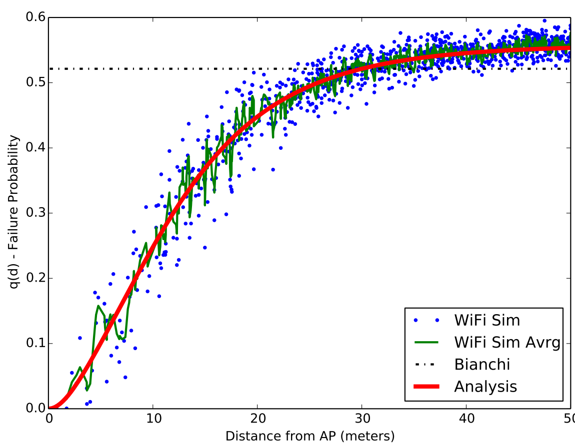

Fig. 3: Failure prob., $q(d)$, for $N = 20$, $H_b = 10\ dB$.

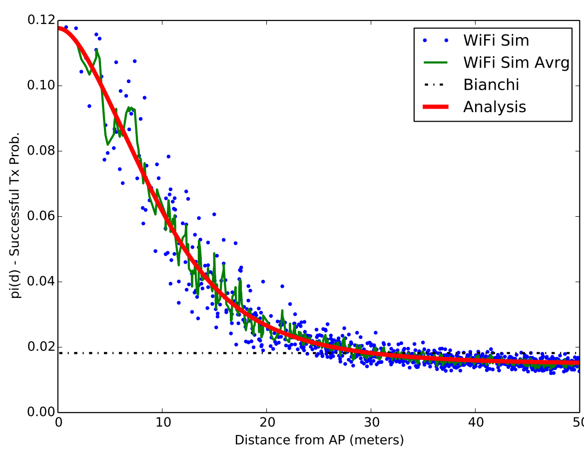

Fig. 4: Successful trans. prob., $\pi(d)$, for $N = 20$, $H_b = 10\ dB$.

VI. Simulations

A. Comparison of Simulation Results and Analytic Results

Simulation settings: We constructed an IEEE 802.11a/g network simulator[4] that simulates the physical channel behavior including the capture effect presented in Section II. We set the contention window to $W = CW_{min} = 16$, $CW_{max} = 256$, i.e., $K = 4$. The attenuation exponent is set to $\alpha = 3$. The AP transmission range is set to $R = 50$ meters. We focus on two probabilities: the expected failure probability, $q(d)$, and successful transmission probability, $\pi(d)$.

The case of uniform user distribution: To validate the accuracy of our analytic model, we compared the simulation results with the analytic results for the case of uniform user distribution. While we used numerous settings, we include only one setting in the paper, shown in Figures 3 and 4, where $N = 20$, $H_b = 10\ dB$ (e.g., the IEEE 802.11a threshold for decoding packets with bit-rate of 18 $Mbps$) and the scale parameter $\sigma = 1.0$, as suggested in Section V. A total of 50 simulation runs are executed, each one with 20 uniformly distributed users. This means that we collected 1000 samples of $q(d)$ and $\pi(d)$. These values are represented as blue dots on the graphs. For higher readability, we grouped individual sample points into average values. The weighted average of five adjacent points along the distance (two before and two after the point at location d) is computed, where the weights of the five points are set to $\{0.1, 0.2, 0.4, 0.2, 0.1\}$. The results of this averaging process are depicted as solid green lines. Finally, the solid red lines are calculated by using our analytic model. The two graphs show very high correlation between the analytic results and the simulation results. The doted black lines are the results of applying the Bianchi model [4].

B. Discussion on Key Factors of Capture Effects

Impact of the number of users (N): Figures 5(a) and 5(b) show the analytic results for various number of users from 5 to 50, where $H_b = 10\ dB$ and $\sigma = 1.0$. As expected, Figure 5(a) shows that the failure probability, $q(d)$, increases as the number of users increases. Regardless of the number of users, the users that are very close to the AP experience very low failure probability, close to zero.

The ratio $\frac{max\{\pi(d)\}}{min\{\pi(d)\}}$, which indicates the ratio between the maximal and the minimal observed bandwidth, can exceed 10. Interestingly, $\pi(d = 0) \approx 12\%$ regardless of the number of users. Since $q(0) \approx 0$, from Eq. (6) and Eq. (7), we learn that

$$\pi(0) = p_{tx}(0) \cdot [1 - q(0)] = \frac{2}{1 + W} \cdot 1 = \frac{2}{17} \approx 12\%$$

[4][13] shows that the capture effect is not accurately simulated by popular simulators such as *ns-2* and *Qualnet*.

Impact of the distance from AP (d): We observe that the failure probability sharply increases as the distance to the AP increases, until a certain point. Beyond this knee point, the failure probability starts to converge (i.e., a plateau). Eq. (20) characterizes this knee point, denoted by $\hat{d}(H_b, R)$.

$$\hat{d}(H_b, R) = \frac{R}{H_b^{1/\alpha}} \quad (20)$$

To understand this knee point, one should observe that, if we ignore fast-fading, i.e., $\sigma = 0$, for any distance $d > \hat{d}$ from the AP the number of interfering nodes does not change. Consider again Eq. (13). Since $\sigma = 0$, $\mathcal{Z}$ is not a random variable and its value is always 0. Thus, $Prob\{Z < g_b(r_s, r_i)\}$ is 1 if $g_b(r_s, r_i) \geq 0$ and it is zero otherwise. $g_b(r_s, r_i) = 0$ if the ratio $\frac{d_s}{d_i} = H_b^{-1/\alpha}$. This means that node i interferes the transmission of node s only if $d_i < d_s \cdot H_b^{1/\alpha}$. Since the maximal distance of a user from the AP is R, by replacing d_i with R, we get the following. If $d_s \geq \hat{d}(H_b, R) = R/H_b^{1/\alpha}$, any simultaneous transmission interferes the transmission of user s, which justifies Eq. (20). For our current settings, $\hat{d}(10\ dB,\ 50\ m) = 23\ m$.

The impact of capture threshold (H_b): Figure 5(c) illustrates our analysis for various capture thresholds, H_b, when the number of users is $N = 20$ and $\sigma = 1.0$. Interestingly, the charts show that H_b does not affect the ratios $\frac{max\{q(d)\}}{min\{q(d)\}}$ and $\frac{max\{\pi(d)\}}{min\{\pi(d)\}}$, which indicates that the worst spatial unfairness (i.e., between the closest user and the farthest user) does not change. However, as we increase H_b, the knee point $\hat{d}(H_b, R)$ is shifted to the left according to Eq. (20).

VII. Conclusion

In this paper, we analyze the long-term unfairness among the users in the IEEE 802.11 network. We experimentally demonstrated that the unfairness occurs even if all users use the same transmission bit rate. The main cause of this unfairness is the capture effect and its interplay with the IEEE 802.11 DCF MAC protocol. We present a mathematical model to accurately estimate the degree of unfairness which is determined by several factors. The accuracy of our model is validated via extensive simulations and experimental measurement. From this validation process, we have obtained several interesting insights on the characteristics of the capture effect in the IEEE 802.11 network. One of the key new findings is that there exists a distance from the AP (which we called a knee point) which decides the impact of the capture effect on the unfairness. We can mathematically predict this point.

In the future, we extend our analytic model to the case when the users transmit with different transmission bit rates. We also plan to explore solutions for mitigating the unfairness.

Acknowledgment

This work was partially supported by the National Research Foundation of Korea(NRF) grant funded by the Korea government(MSIP) (No. 2013R1A2A2A01068325).

References

[1] M. Heusse, F. Rousseau, G. Berger-Sabbatel, and A. Duda, *Performance Anomaly of 802.11b*, *IEEE Infocom*, 2003.

[2] J. Manweiler, N. Santhapuri, S. Sen, R. Roy Choudhury, S. Nelakuditi, K. Munagala, *Order matters: Transmission reordering in wireless networks*, *IEEE/ACM Tr. on Networking* 20 (2), 2012, pp. 353 366.

[3] P. Patras, H. Q and D. Malone, *Mitigating Collisions through Power-Hopping to Improve 802.11 Performance*, *Elsevier Pervasive and Mobile Computing*, 11, April 2014, pp. 41–55.

[4] G. Bianchi, *Performance analysis of the IEEE 802.11 distributed coordination function*, *IEEE JSAC*, Vol. 18(3), March 2000.

[5] H. Chang, V. Misra, D. Rubenstein, *A General Model and Analysis of Physical Layer Capture in 802.11 Networks*, *IEEE Infocom*, 2006.

[6] Z. Hadzi-Velkov and B. Spasenovski, *Capture effect in IEEE 802.11 basic service area under influence of Rayleigh fading and near/far effect*, *IEEE PIMRC*, 2002.

[7] F. Daneshgaran, et.al., *Saturation throughput analysis of IEEE 802.11 in presence of non-ideal transmission channel and capture effects*, *IEEE Tr. on Communications*, Vol. 56(7), 2008.

[8] F. Daneshgaran, et.al., *Unsaturated throughput analysis of IEEE 802.11 in presence of non-ideal transmission channel and capture effects*, *IEEE Tr. on Wireless Communications*, Vol. 7(4), 2008.

[9] H. Han, Z. Pei, W. Zhu, and N. Li, *Saturation Throughput Analysis of IEEE 802.11 b DCF Considering Capture Effects*, *IEEE WiCOM*, 2012

[10] G. Sutton, R. Liu, and I. Collings, *Modelling IEEE 802.11 DCF Heterogeneous Networks with Rayleigh Fading and Capture*, *IEEE Transactions on Communications*, Vol. 61(8), 2013.

[11] M. Zorzi and R.R. Rao, *Capture and retransmission control in mobile radio*, *IEEE JSAC*, Vol. 12(8), Oct 1994.

[12] C. Ware, J. Judge, J. Chicharo, and E. Dutkiewicz, *Unfairness and capture behaviour in 802.11 adhoc networks*, *IEEE ICC*, 2000.

[13] A. Kochut, A. Vasan, A. U. Shankar, and A. Agrawala, *Sniffing out the correct physical layer capture model in 802.11b*, *IEEE ICNP*, 2004.

[14] J. Lee, et.al., *An Experimental Study on the Capture Effect in 802.11a Networks*, ACM WinTech, 2007.

[15] S. Ganu, et.al., *Methods for restoring MAC layer fairness in IEEE 802.11 networks with physical layer capture*, ACM REALMAN, 2006.

[16] L. Luo, M. Gruteser and H. Liu, *Achieving Temporal Fairness in Multi-Rate 802.11 WLANs with Capture Effect*, *IEEE ICC*, 2009.

[17] S. Han, T. Nandagopal, Y. Bejerano, and H. Choi, *Analysis of Spatial Unfairness in Wireless LANs*, *IEEE Infocom*, 2009.

[18] B. O'Hara and Al Petrick, *The IEEE 802.11 Handbook: A Designer's Companion, 2nd Edition*, IEEE press, 2005.

[19] T. S. Rappaport, *Wireless Communication Principle and Practice*. Prentice Hall, 1996.

[20] A. Goldsmith, *Wireless Communication*. Cambridge Univ. Press, 2005.

[21] Robert Akl, Dinesh Tummala and Xinrong Li, *Indoor Propagation Modeling At 2.4 Ghz for IEEE 802.11 Networks*, Sixth IASTED International Multi-Conference on Wireless and Optical Communications, 2006.

[22] Cisco Aironet 802.11a/b/g Wireless CardBus Adapter http://www.cisco.com/c/en/us/products/collateral/wireless/aironet-802-11a-b-g-cardbus-wireless-lan-client-adapter-cb21ag/product_data_sheet09186a00801ebc29.html